Journal of Alloys and Compounds 509S (2011) S754–S758

Contents lists available at ScienceDirect

Journal of Alloys and Compounds

journal homepage: www.elsevier.com/locate/jallcom

Effect of mechanically induced modification on TiH_2 thermal stability

O.S. Morozova[a,*], T.I. Khomenko[a], Ch. Borchers[b], A.V. Leonov[c]

[a] Semenov Institute of Chemical Physics RAS, Kosygin st. 4, 119991 Moscow, Russia
[b] Institute of Material Physics, University of Goettingen, Friedrich-Hund-Platz 1, 37077 Goettingen, Germany
[c] Lomonosov Moscow State University, Chemical Department, Leninskie Gory, 119899 Moscow, Russia

ARTICLE INFO

Article history:
Received 11 August 2010
Received in revised form
30 December 2010
Accepted 7 January 2011
Available online 20 January 2011

Keywords:
TiH_2 as-milled
TiH_2/B and TiH_2/C nanocomposites
Ball-milling treatment
High-resolution transmission electron microscopy
Interrupted temperature programmed desorption
X-ray diffraction

ABSTRACT

Interrupted thermal desorption and X-ray diffraction techniques were used to study the effect of graphite and boron additives on non-equilibrium decomposition of mechanically activated commercial TiH_2. The phase transformation sequence is described as a number of consecutive reactions corresponding to desorption peaks. The process is compared to non-equilibrium decomposition of commercial TiH_2. The mechanical pre-treatment with additives significantly eases and accelerates decomposition of TiH_2 to αTi(H), but hinders the stage of αTi(H) → αTi transformation. Only a small portion of pure αTi was detected for as-milled TiH_2 and TiH_2/B powders after the final TPD. No αTi was formed in the case of as-milled TiH_2/C.

1. Introduction

The major requirements for metal hydrides as hydrogen storage materials are the high hydrogen mass percentage, chemical stability and low-temperature fast hydrogenation and dehydrogenation kinetics [1]. The charging–discharging kinetics can be significantly improved by ball milling treatment of the powders in the presence of different additives [2–4]. Non-equilibrium heating conditions in the temperature programmed desorption (TPD) regime accelerate the metal hydride decomposition procedure. As was shown by the example of TiH_2, ball-milling with graphite, boron and h-BN additives [5,6] drastically decreases Ti-hydride decomposition temperature in TPD regime due to (1) powder size degradation and (2) appearance of new occupation sites available for H atoms in TiH_2 lattice modified by C, B, and N interstitial atoms, respectively. However, this non-equilibrium metal hydride decomposition is a poorly studied multi-stage process, the single stages of which can be accelerated or retarded by different pretreatment procedures [7].

This study is focused on the mechanism of non-equilibrium decomposition of ball-milled commercial TiH_2 compared to that of original Ti-hydride [8], and on the effect of boron and graphite additives on this process. The phase transformation sequence is depicted as a number of consecutive and parallel reactions.

2. Experimental

Commercial TiH_2 (Aldrich, 99% pure, 325 mesh, $S = 0.32\ m^2/g$), boron (amorphous, purity: 98.5%, $S = 5.4\ m^2/g$) and graphite (highly oriented pyrolytic, purity: 99%, $S = 3\ m^2/g$) powders were used. 16.6 mass% of boron or graphite was added to TiH_2. Milling was carried out for 66 min at the room temperature in a flow mechanochemical reactor with an average power intensity of 1 W/g in He flow. The TiH_2 decomposition was studied by temperature-programmed desorption (TPD) technique. Peaks were separated according to Lorentzian TPD curve fitting. The experimental details are published elsewhere [5]. The sample was heated up to the chosen temperature and then rapidly cooled by transferring the reactor from the heater to ice water. A fresh powder was used in each TPD run. XRD patterns were recorded after each TPD experiment using a Dron-3 diffractometer with Cu Kα radiation. Quantitative X-ray phase analysis was performed applying a fitting procedure [9].

3. Results and discussion

Significant TiH_2 powder size degradation accompanied by partial hydrogen loss was observed during the mechanical treatment (Fig. 1). TiH_2, TiH_2/C and TiH_2/B powders lost approximately

* Corresponding author at: Department of Kinetics and Catalysis, Semenov Institute of Chemical Physics RAS, Kosygin st. 4, 119991 Moscow, Russia. Tel.: +7 495 939 7195; fax: +7 495 651 2191.
E-mail address: om@polymer.chph.ras.ru (O.S. Morozova).

0925-8388/$ – see front matter © 2011 Elsevier B.V. All rights reserved.
doi:10.1016/j.jallcom.2011.01.048

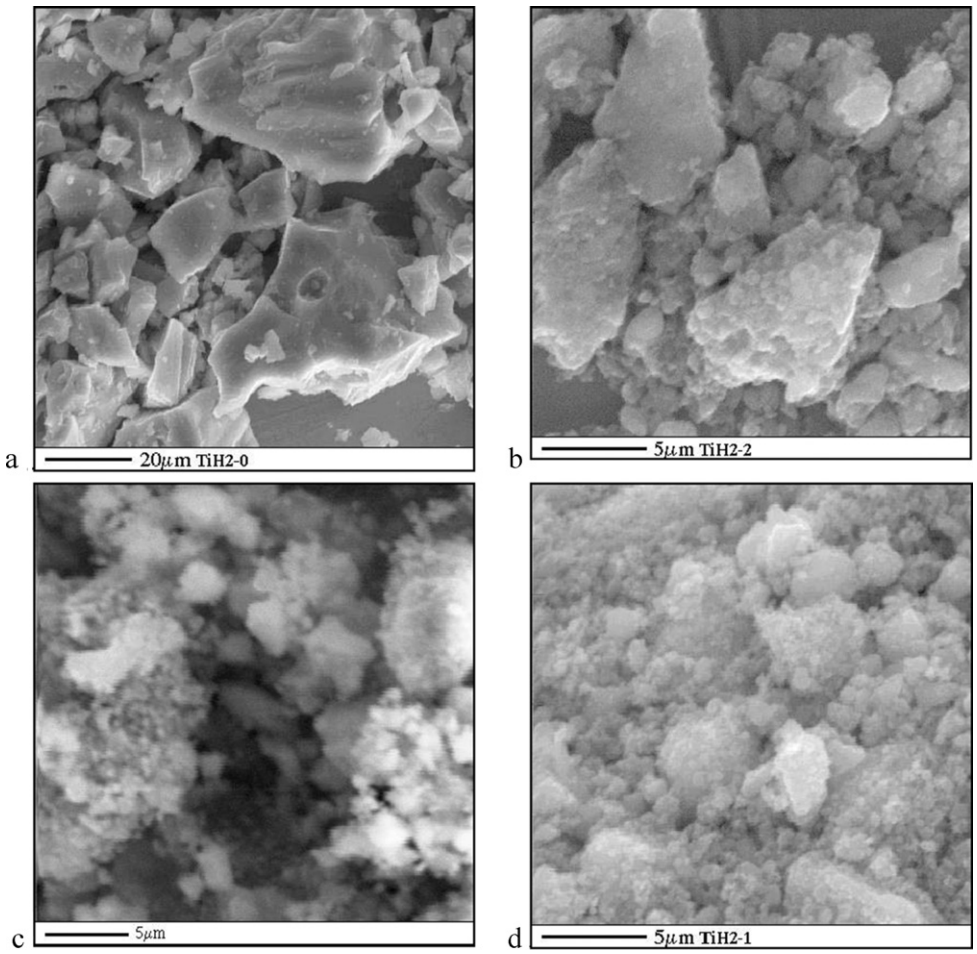

Fig. 1. SEM micrograph: (a) commercial TiH_2; (b) TiH_2 milled for 66 min; (c) TiH_2/B milled for 66 min; (d) TiH_2/C milled for 66 min.

~5 at.%, ~6 at.%, and ~14 at.%, respectively, after 66 min of milling. As a result, $TiH_{1.9}$, $TiH_{1.88}$/C and $TiH_{1.72}$/B emerged. Accordingly, the specific surface area increased from 0.32 m^2/g to 6 m^2/g, 38.2 m^2/g and 6 m^2/g for TiH_2, TiH_2/C and TiH_2/B, respectively. Average grain size (from Scherer formula) was 13–15 nm. Fig. 2 shows TPD curves recorded for TiH_2 original and as-milled powders. Desorption in the low-temperature region is a special feature of as-milled powders: H_2 release was detected at 300–350 K, which is remarkably lower than original TiH_2 onset temperature. Hydrogen desorption during TPD was accompanied by structural transformations of TiH_2 up to total decomposition. Step-by-step correlation between both processes was studied by XRD, see Fig. 3.

The decomposition of original TiH_2 was recently studied in detail [8]. According to XRD data (Fig. 3a), the total decomposition of original TiH_2 was divided into three parts corresponding to three peaks that could be fitted to the TPD spectrum (Fig. 2a): (1) $\varepsilon TiH_2 \rightarrow \delta TiH_{2-x}$ transition at T_{max} = 743 K, (2) $\delta TiH_{2-x} \rightarrow \alpha Ti(H)$ at T_{max} = 817 K and (3) $\alpha Ti(H) \rightarrow \alpha Ti$ at T_{max} = 925 K. Finally, original εTiH_2 was totally decomposed to αTi. According to Ti–H phase diagram, the presence of βTi (the high-temperature phase) should be postulated. But, it was not detected by XRD.

Figs. 2b and 3b show TPD spectrum and XRD patterns recorded for as-milled TiH_2. The low-temperature part of TPD curve was attributed to the fast transformation $\delta TiH_{2-x} \rightarrow \alpha Ti(H)$. Approximately 50% of H_2 was desorbed during the heating to 723 K. As a result, ~50 wt.% of δTiH_{2-x} was decomposed to a solid solution αTi–9 at.% H. The lattice constant of residual δTiH_{2-x} decreased from a = 0.444 nm to a = 0.441 nm indicating a decrease in hydrogen content [10]. Further heating stimulated both αTi(H) formation and progressive decrease of hydrogen content in δTiH_{2-x}. The high-temperature peak with T_{max} = 795 K is mainly reflecting the decomposition $\alpha Ti(H) \rightarrow \alpha Ti$. After final heating, the sample consists of about 83 wt.% of αTi–6 at.% H and αTi. The data obtained are in a good agreement with [7].

Figs. 2c and 3c show TPD spectrum and corresponding XRD patterns of TiH_2/B powder. TiH_2 decomposition started at about 300 K. The major low-temperature process was $\delta TiH_{2-x} \rightarrow \alpha Ti(H)$ accompanied by a decrease of hydrogen content in both δTiH_{2-x} and αTi(H) lattices. Thus, heating to 689 K led to H_2 loss of ~ 47 mol.%. As a result, about 37 wt.% of hexagonal solid solution αTi–11.4 at.% H (a = 0.298 nm, c = 0.481 nm) was detected. Such a hydrogen concentration exceeds the equilibrium concentration of 8.4 at.% H [10] by far. Besides, δTiH_{2-x} lattice parameter decreased from 0.444 nm to 0.442 nm due to a depletion of hydrogen in Ti-hydride. Heating to 742 K led to about 66 mol.% H_2 loss and further $\delta TiH_{2-x} \rightarrow \alpha Ti(H)$ transformation accompanied by narrowing and large-angle shift of XRD peaks of both phases. The hydrogen content in αTi(H) solid solution decreased to 9–10 at.% (a = 0.297 nm, c = 0.481 nm), which still exceeds the equilibrium concentration. The high-temperature TPD peak (T_{max} = 759 K) reflects the decomposition $\delta TiH_{2-x} \rightarrow \alpha Ti(H) \rightarrow \alpha Ti$. The major phase present after heating to 822 K was a solid solution αTi–7.4 at.% H (a = 0.297 nm; c = 0.477 nm). Only traces of δTiH_{2-x} were detected. The high temperature slope reflects the transformation $\alpha Ti(H) \rightarrow \alpha Ti$: the final product of heating to 945 K contained traces of αTi and two hexagonal phases characterized by equal parameters a = 0.296 nm and

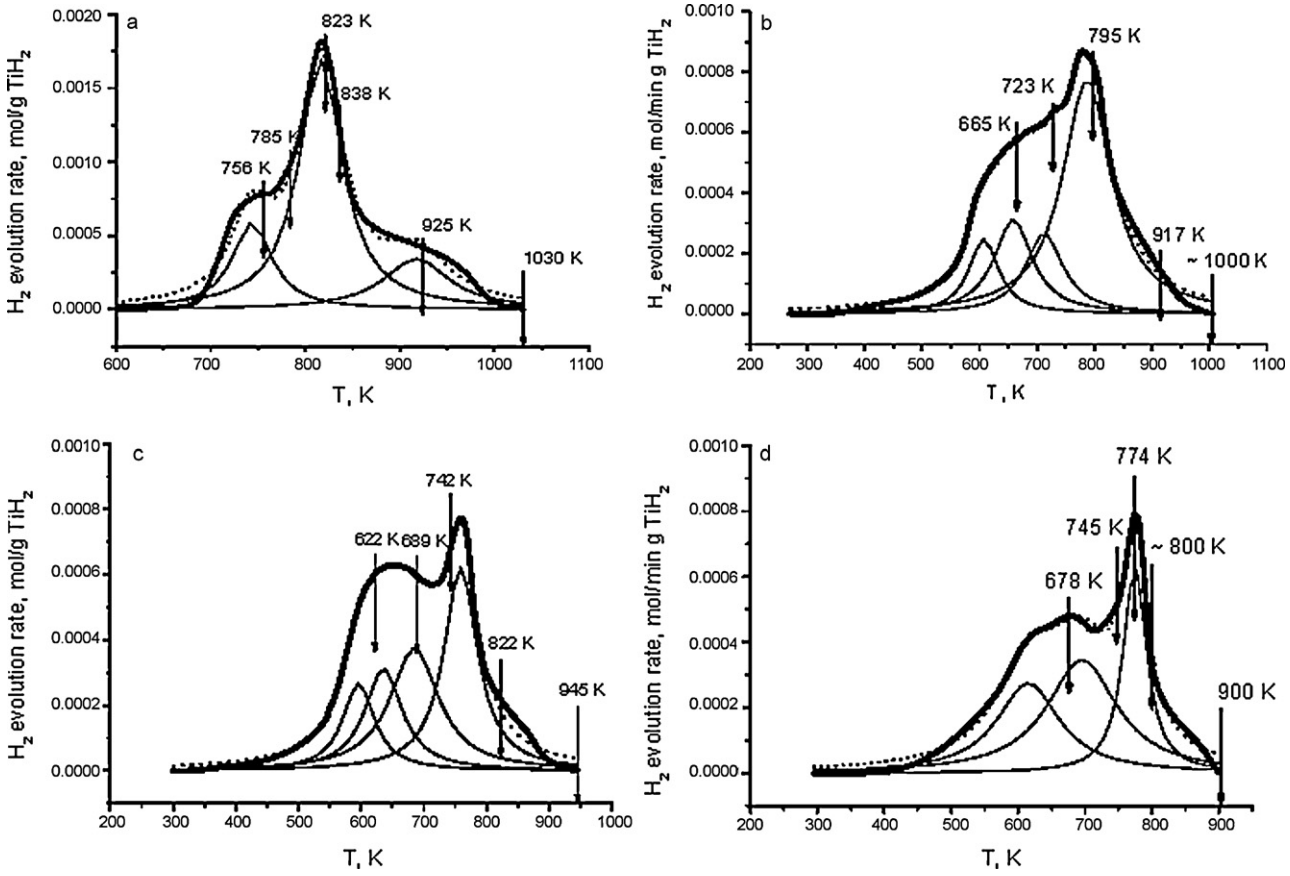

Fig. 2. TPD spectra recorded for (a) commercial TiH_2 [8] and as-milled: (b) TiH_2, (c) TiH_2/B, and (d) TiH_2/C. Vertical arrows point to temperatures of heating interruption.

different $c = 0.471$ nm and $c = 0.478$ nm, respectively. The first phase was attributed to αTi–1.6 at.% H. Since hydrogen evolution was virtually finished, the second hexagonal phase was attributed to a solid solution αTi(B), which was confirmed by XES technique [6]. Residual hydrogen was totally released after heating to 1073 K. The hexagonal phase αTi–1.6 at.% H disappeared, and the hexagonal solid solution αTi(B) and a rather dispersed cubic phase TiB ($a = 0.421$ nm) were detected.

Figs. 2d and 3d show TPD and XRD spectra for TiH_2/C powder. TiH_2 decomposition also started at ~300 K by the transformation $\delta TiH_{2-x} \rightarrow \alpha Ti(H)$, a solid solution with a non-equilibrium H content up to 9 at.%. At 774 K, the major phase was a solid solution αTi(H). Only traces of δTiH_{2-x} were detected. The high-temperature slope of TPD peak with $T_{max} = 774$ K reflected two processes: the evolution of residual hydrogen and the formation of Ti(C,H) solid solutions. According to mass balance and XRD data, the final product formed at 900 K consisted of two hexagonal phases (αTi – 8 at.% H and αTi(C)) and a highly dispersed cubic phase Ti(C,H) in an amount of ~32 wt.%. Here we also suppose the carburization of Ti-hydride during hydrogen evolution from Ti-hydride bulk, which may be a result of TiH_2 lattice modification by C atoms under mechanical treatment [5]. Due to graphite excess, a carbon peak is present in XRD patterns.

As was mentioned above, the presence of βTi (the high-temperature phase) should be postulated according to Ti–H phase diagram. But, it was not detected by XRD in the samples cooled on different TPD stages.

Table 1 summarizes the data obtained in TPD experiments and the effective activation energies E_a of H_2 desorption calculated for the first and the last (high-temperature) peaks responsible for initial δTiH_{2-x} decomposition and $\alpha Ti(H) \rightarrow \alpha Ti$ transforma-

Table 1
TPD parameters calculated on a base of Lorentzian fitting of TPD spectra.

Sample	Peak	H_2 evolution [mol/g TiH_2]	T_{max} [K]	E_a [kJ/mol]
TiH_2	1	3.9×10^{-3} (19.5 mol.%)	743	219.5 ± 6.5
	2	1.23×10^{-2} (61.6 mol.%)	817	229.7 ± 7.2
	3	3.8×10^{-3} (18.9 mol.%)	920	216.1 ± 7.3
TiH_2 as-milled	First	2.04×10^{-3} (10.9 mol.%)	607	107.9 ± 5.2
	Last	1.13×10^{-2} (56.4 mol.%)	787	126.3 ± 2.9
TiH_2/B as-milled	First	2.28×10^{-3} (14.3 mol.%)	596	65.4 ± 1.5
	Last	5.6×10^{-3} (35.2 mol.%)	759	170.4 ± 7.3
TiH_2/C as-milled	First	5.46×10^{-3} (~29 mol.%)	614	35.7 ± 0.5
	Last	4.88×10^{-3} (~26 mol.%)	774	209.2 ± 11.9

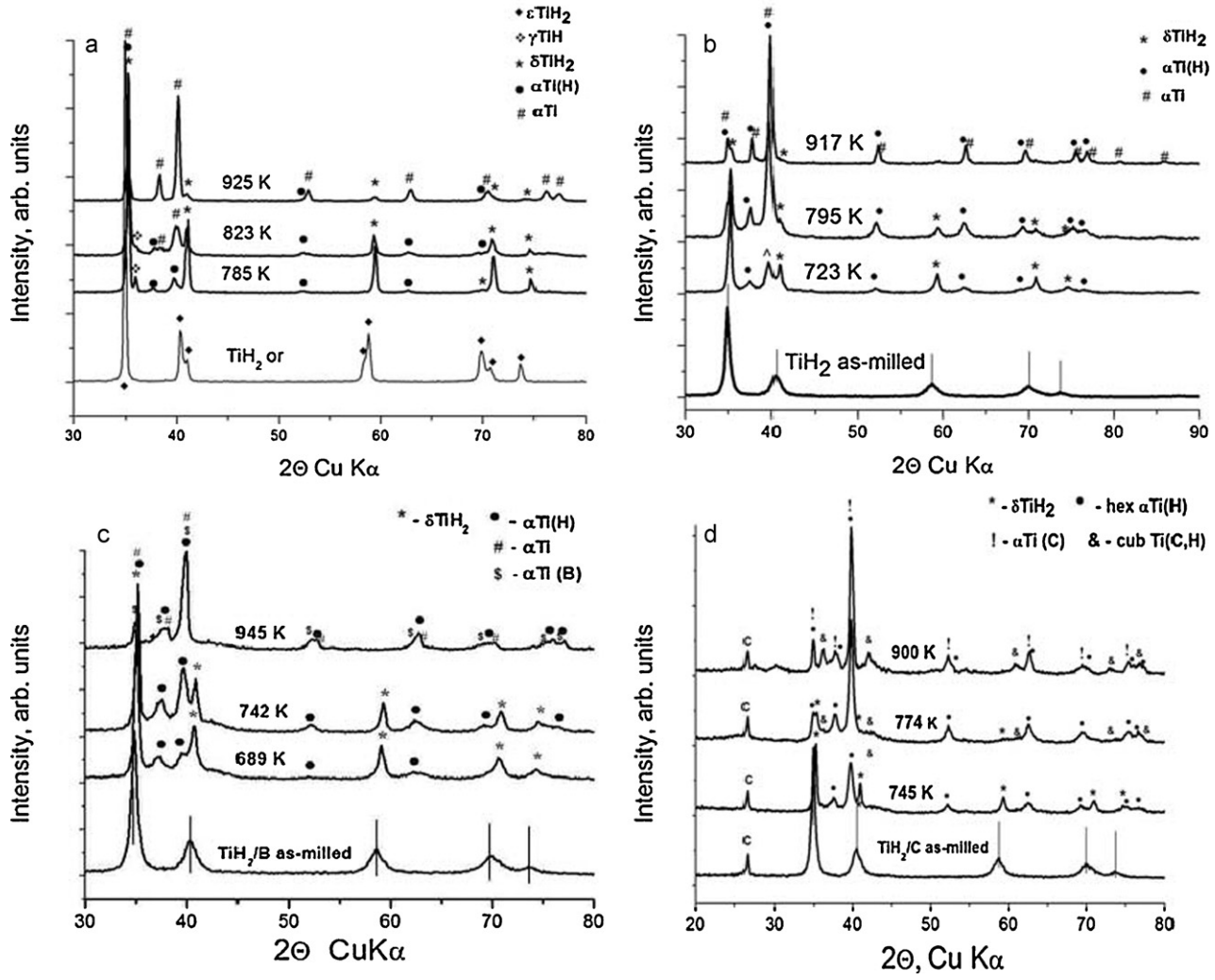

Fig. 3. XRD patterns recorded for TiH_2, TiH_2/B and TiH_2/C powders original, as-prepared and after TPD experiments depicted in Fig. 2: (a) commercial TiH_2, original and heated to785 K (low-temperature slop), 823 K (T_{max} of the major peak) and 925 K (final decomposition) [8]; (b) as-milled TiH_2 original and heated to 723 K (low-temperature slop), 795 K (~T_{max} of the major peak) and 917 K (final decomposition); (c) as-milled TiH_2/B original and heated to 689 K (just after the low-temperature T_{max}), 742 K (nearby ~T_{max} of the high-temperature peak) and 945 K (final decomposition); (d) as-milled TiH_2/C original and heated to 745 K (after the low-temperature T_{max}), 774 K (~T_{max} of the high-temperature peak) and 900 K (final decomposition).

tion, respectively. The processes include diffusion of H atoms from the bulk to the surface, surface recombination of H atoms and H_2 desorption itself. Nevertheless, our estimations are in a good agreement with experiment: E_a corresponding to the first process (at around 600 K) drastically decreases in the order TiH_2, TiH_2 as-milled, TiH_2/B, TiH_2/C. E_a corresponding to the second process significantly decreases for as-milled sample, but increases again for TiH_2/B, TiH_2/C. This effect is likely to be related to the growth of the fraction of highly distorted intergrain regions in nanocomposite TiH_2/B and TiH_2/C powders, where H mobility is much lower than in the crystalline grains [11] or caused by difficulties in H atoms recombination on the surfaces blocked by boron or carbon.

4. Conclusions

The mechanical activation of TiH_2 and, in particular, mechanical activation with graphite and boron additives enhances Ti-hydride decomposition kinetics to hexagonal solid solution T(H) because: (1) one stage of this process $\varepsilon TiH_2 \rightarrow \delta TiH_{2-x}$ was eliminated, (2) initial E_a of hydrogen desorption at low temperatures dramatically decreased and (3) B and C atoms modified activated δTiH_{2-x} lattice of to give αTi(B) or Ti-carbide-like phases. In contrast, it suppresses αTi(H) → αTi decomposition due to high concentration of structural defects and strong affinity of hydrogen to boron and carbon, reflected by a pronounced increase in effective E_a of hydrogen desorption.

Acknowledgements

This work was partly supported by Russian Foundation of Basic Research (Project No. 10-03-00942-a) and Ministry of Science of Russian Federation (Contract No 02.740.11.5176).

References

[1] A. Zaluska, L. Zaluski, J.O. Ström-Olsen, Appl. Phys. A 72 (2001) 157–165.
[2] R.A. Varin, S. Li, A. Calka, D. Wexler, J. Alloys Compd. 373 (2004) 270–276.
[3] H. Imamura, N. Takashi, T. Fujinaga, J. Alloys Compd. 253–254 (1997) 34–37.
[4] C.Z. Wu, P. Wang, X. Yao, C. Liu, D.M. Chen, G.Q. Lu, H.M. Cheng, J. Alloys Compd. 414 (2006) 259–264.
[5] E.Z. Kurmaev, O.S. Morozova, T.I. Khomenko, Ch. Borchers, S.N. Nemnonov, Y. Harada, T. Tokushima, H. Osawa, T. Takeuchi, S. Shin, J. Alloys Compd. 395 (2005) 240–246.

[6] O.S. Morozova, T.I. Khomenko, A.V. Leonov, Ch. Borchers, E.Z. Kurmaev, A. Moewes, J. Alloys Compd. 483 (2009) 309–312.
[7] V. Bhosle, E.G. Baburaj, M. Miranova, K. Salama, Mater. Sci. Eng. A356 (2003) 190–199.
[8] Ch. Borchers, T.I. Khomenko, A.V. Leonov, O.S. Morozova, Termochim. Acta 493 (2009) 80–84.
[9] E.V. Shelekhov, T.A. Sviridova, Met. Sci. Heat Treat. 42 (2000) 309.
[10] F.D. Manchester, A. San-Martin, The H–Ti (hydrogen–titanium) system, in: F.D. Manchester (Ed.), Phase Diagrams of Binary Hydrogen Alloys, ASM International, USA, 2000, pp. 238–258.
[11] A.Ye. Yermakov, N.V. Mushnikov, M.A. Uimin, V.S. Gaviko, A.P. Tankeev, A.V. Skripov, A.V. Solonin, A.L. Buzlukov, J. Alloy Compd. 425 (2006) 367–372.